AIChE WILEY InterScience DISCOVER SOMETHING GREAT

FLUID MECHANICS AND TRANSPORT PHENOMENA

# Dynamics of Particles Suspended in a Yield Stress Fluid Flowing in a Pipe

**Othmane Merkak, Laurent Jossic, and Albert Magnin**
Laboratoire de Rhéologie, Domaine Universitaire, B.P. 53, 38041 Grenoble, Cedex 9, France
and
Université Joseph Fourier Grenoble 1, Institut National Polytechnique de Grenoble, CNRS UMR 5520, 38041 Grenoble, Cédex 9, France

*DOI 10.1002/aic.11454*
*Published online February 29, 2008 in Wiley InterScience (www.interscience.wiley.com).*

*This study seeks to understand the basic mechanisms governing the dynamics of a solid particle in a Poiseuille flow field of a viscoplastic fluid. An experimental set-up to create flows with a prescribed flow rate and enable the particles to be visualized in three dimensions was designed and validated. The absence of slip at the interfaces between flows and particles was characterized. The Reynolds numbers are low, gravity effects negligible and plastic effects significant. The ratio of pipe diameter to particle diameter is 8. The dynamics of a particle in a velocity field depends strongly on its position in the sheared wall zone or in the moving rigid zone. The effect of rigid and sheared zones on particle behavior was examined. Changes in particle translation and rotation velocities were quantified.* © 2008 American Institute of Chemical Engineers *AIChE J,* 54: 1129–1138, 2008

*Keywords: suspensions, yield stress fluid, laminar flow, rheology*

## Introduction

Many industrial applications involve flows of suspensions of solid particles in a gelled yield stress fluid. This is the case particularly in the oil industry with drilling slurry, and in the food processing industry, where many products have small pieces suspended in a gelled suspending matrix. Another example, from the building industry, is that of concrete. Although the stakes are high, there is little information on this subject in the literature. The behavior of these materials when flowing is still poorly controlled. Jossic et al.[1–3] demonstrated new migration and segregation phenomena that generate particular structures. To understand and control the basic mechanisms of these phenomena more completely, this study focuses on the dynamics of a solid particle in the shear field of a viscoplastic fluid flowing with very low inertia in a cylindrical pipe. In addition, as the ratio of the diameter of the pipe to that of the particle is small, the influence of the wall can never be neglected.

In the case of a Newtonian suspending fluid, the literature is abundant concerning the behavior of a sphere in a shear field or relatively concentrated suspensions.[4–15] Matas et al.[16] recently summarized the main conclusions of these results. In a word, the main point to be borne in mind is that the migration of a particle in a flow is a nonlinear phenomenon. This nonlinearity may be the result of inertia, interactions between spheres, or the non-Newtonian character of the fluid. Thus, with a Reynolds number of 0, the Stokes equations, which are linear, predict that a solid particle cannot undergo any lateral migration in a Newtonian fluid. With low but non-zero Reynolds numbers, Segré and Silberberg[4] demonstrated the existence of an equilibrium position situated at $r = 0.62R$ for neutrally buoyant spheres. This equilibrium position is the result of competition between a repulsion force due to the walls and a force due to the curvature of the shear field. If the difference in density between the sphere and the fluid is other than zero, the Saffman force modifies the equilibrium position. It moves towards the walls when the sphere is denser (resp. less

Correspondence concerning this article should be addressed to A. Magnin at magnin@ujf-grenoble.fr.

dense) than the fluid in descending (resp. ascending) flow. In contrast, the equilibrium position is closer to the axis when the sphere is denser (resp. less dense) than the fluid in an ascending (resp. descending) flow. Table 1 is an updated version of the table given by Brenner,[9] summarizing the main results.

There are far fewer results for the case of a complex non-Newtonian fluid. The main ones are those obtained by Karnis and Mason[17] and by Gauthier et al.[18] The latter dealt with the phenomenon of lateral migration in the case of a pseudoplastic fluid. They showed that a rigid spherical particle migrates towards the wall. In the case of an elastoplastic fluid, they showed that the particles migrate towards the centre line of the pipe. There are still very few studies concerning the case of yield-stress suspending fluids. Jossic et al.[1–3] observed segregation and migration phenomena in laminar flows with low Reynolds numbers.

To gain further knowledge in this field, this study looks at the more fundamental case of the dynamics of spherical particles in suspension in a viscoplastic fluid, flowing in a horizontal cylindrical pipe. Inertia and gravity effects are negligible. The solid particles and fluid have very similar densities. At rest the spherical particles are highly stabilized by the yield-stress matrix.

An experimental set-up was designed and instrumented to display the particle trajectories in the three dimensions of space during flow. Head losses were also measured. Careful attention was paid to controlling flow and particle slip at the wall during both the rheometric characterizations and experiments in the pipe.

The motion of a particle, characterized by its translation velocity $U_T$ and its rotation velocity $\Omega$, were studied at various positions in the pipe and with different flow velocities. Physical explanations are proposed for the phenomena observed. This study helps to extrapolate the results obtained in order to understand and explain the most complex cases so that they can be better controlled.

## Theoretical Approach

The suspensions studied here consist of rigid spheres and a gelled model fluid. The fluid is a gel considered to be viscoplastic, with a rheological behavior obeying the Herschel-Bulkley model:

$$\begin{cases} \underline{\underline{\tau}} = 2\left(K\sqrt{-4D_{II}}^{n-1} + \dfrac{\tau_0}{\sqrt{-4D_{II}}}\right)\underline{\underline{D}} & \text{if } -\tau_{II} > \tau_0^2 \\ \underline{\underline{D}} = 0 & \text{if } -\tau_{II} \leq \tau_0^2 \end{cases} \quad (1)$$

with $\tau_0$ being the yield stress, $K$ the consistency index, $n$ the power-law index, $\underline{\underline{D}}$ the rate of strain tensor, $\underline{\underline{\tau}}$ the extra stress tensor, $II$ the second invariant of corresponding tensor. However, it should be noted that the model fluid used in this study has an elastoviscoplastic behavior (see the section on Material and Rheometry).

The flow of a yield-stress fluid in a cylindrical pipe generates a velocity profile made of a plug flow zone near the centre line, where stresses are below the yield-stress, and a sheared zone close to the walls, where stresses are above the yield-stress, Figure 1. The radius of the plug flow zone, or

**Table 1. °Behavior of a Particle Under Flow in a Cylindrical Pipe; Comparison with Main Results of Literature**

| Authors | Flow | Fluid | Study | $1/d$ | $Re$ | $\Delta\rho$ | Concentration | Results |
|---|---|---|---|---|---|---|---|---|
| Segré and Silberberg (1962b)[1] | Vertical | Newtonian | Experimental | 1/36 − 1/7 | 2–30 | $\Delta\rho = 0$ | Dilute suspension | Migration of the particle towards equilibrium position (0.63*R*) from centre line. |
| Goldsmith and Mason (1962)[3] | Horizontal | Newtonian | Experimental | 1/8 − 1/7 | $0.8 \times 10^{-3}$–$1.6 \times 10^{-3}$ | $\Delta\rho = 0$ | One sphere | No radial migration of the particles. |
| Cox and Mason (1971)[9] | Vertical | Newtonian | Experimental | 1/38; 1/18; 1/9 | $<10^{-3}$ | $\Delta\rho = 0$ | Dilute 0.14 and 0.34 | No radial migration of the particles.<br>Rotation of the particles located near the walls.<br>Transfer of the particles located in the central zone of the cylindrical pipe. |
| Gauthier, Goldsmith, and Mason, (1971)[14] | Vertical | Pseudoplastic | Experimental | $\neq 1/d$ | $<10^{-5}$ | $\Delta\rho = 0$ | Very dilute | Migration of the particle towards the pipe wall. |
| | Vertical | Elastoviscous | Experimental | $\neq 1/d$ | $<10^{-5}$ | $\Delta\rho = 0$ | suspension | Migration of the particle towards the cylinder centre line. |
| Feng, Hu, and Joseph (1994)[10] | Vertical | Newtonian | Numerical | 1/4 | $Re \approx 40$ | $\Delta\rho = 0$ | One sphere | Migration of the particle towards equilibrium position (0.63R) from centre line. |
| Jossic, Briguet, and Magnin (2002)[15] | Horizontal | Viscoplastic | Experimental | 1/4 | $7 \times 10^{-8}$–$8 \times 10^{-5}$ | $\Delta\rho \neq 0$ | Dilute 5% and 20% | Migration of the particle towards the top of the cylindrical pipe. |
| Matas, Morris, and Guazzelli, (2004)[12,13] | Horizontal | Newtonian | Experimental | 1/8 − 1/42 | 67–1700 | $\Delta\rho = 0$ | Very dilute suspension 1% | Migration of the particle towards the pipe wall. |
| Present results | Horizontal | Viscoplastic | Experimental | 1/8 | $10^{-6}$–$10^{-3}$ | $\Delta\rho = 0$ | Dilute 1% and 3% | No radial migration of the particles.<br>Rotation of the particles located near the walls.<br>Transfer of the particles located in the central zone of the cylindrical pipe.<br>Particle in contact or very close adhering to pipe wall. |

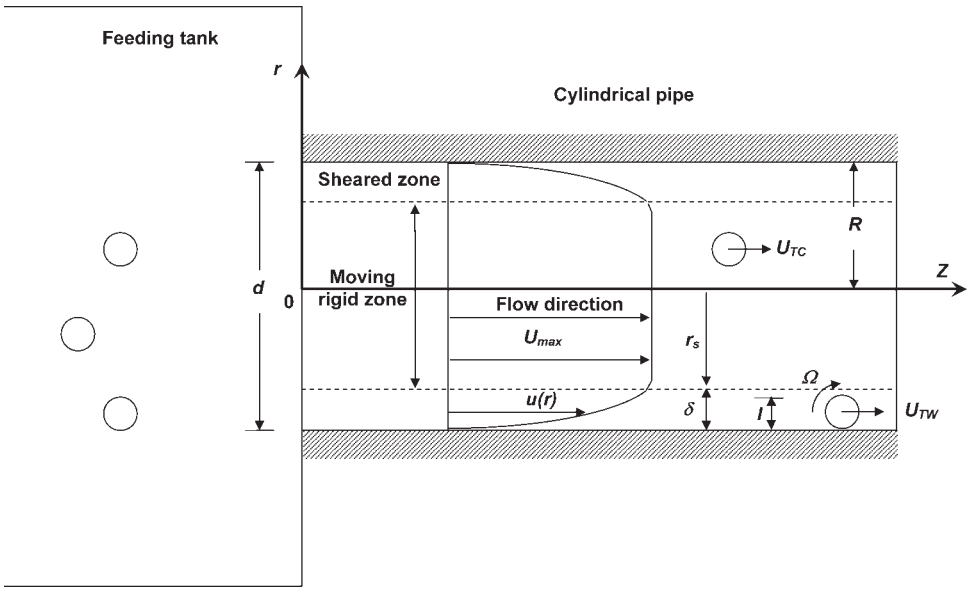


**Figure 1. Velocity profile of a viscoplastic fluid flowing in a cylindrical pipe.**

mobile rigid zone, is designated $r_s$. The thickness of the sheared zone is designated $\delta$ with $\delta = R - r_s$, where $R$ is the radius of the pipe.

The analytical expression of the velocity profile of a Herschel-Bulkley fluid flowing in a cylindrical pipe in steady conditions, Scott-Blair,[19] is:

$$\begin{cases} \dfrac{u(r)}{u} = \dfrac{3n+1}{n+1}\dfrac{(1-a)^{1+\frac{1}{n}} - \left(\frac{r}{R}-a\right)^{1+\frac{1}{n}}}{F(a,n)} & \text{when } 1 \le \dfrac{r}{r_s} \le \dfrac{R}{r_s} \\ \dfrac{u(r_s)}{u} = \dfrac{3n+1}{n+1}\dfrac{(1-a)^{1+\frac{1}{n}}}{F(a,n)} = \dfrac{U_{\max}}{u} & \text{when } 0 \le \dfrac{r}{r_s} \le 1 \end{cases} \tag{2}$$

$a = \tau_0/\tau_w = r/r_s$ is the ratio of the yield stress of the fluid to the stress at the wall $\tau_w$. $u$ designates the average flow velocity. The velocity of the plug flow zone is the maximum velocity of the velocity profile $U_{\max}$. In the case of a Herschel-Bulkley fluid:

$$F(a,n) = (1-a)^{1/n}\left(1 - \frac{a}{2n+1} - \frac{2n}{(n+1)(2n+1)}a^2 - \frac{2n^2}{(n+1)(2n+1)}a^3\right).$$

A similarity study of the flow of a suspension of solid spheres in a viscoplastic fluid flowing in a cylindrical pipe reveals the following dimensionless numbers. They can be used to identify the main effects governing the flow.

The Reynolds number represents the ratio of inertia effects to viscous effects:

$$Re = \frac{\rho_f\, u^{2-n} d^n}{k} \tag{3}$$

$\rho_f$ designates the density of the fluid. In view of the velocities considered in this study, $Re$ is between $10^{-6}$ and $10^{-1}$. Inertia effects are therefore small in relation to viscous effects.

The Oldroyd number[20,21] represents the ratio of plastic forces to viscous forces:

$$Od = \frac{\tau_0}{k(u/d)^n} \tag{4}$$

Shear-thinning is characterized by the flow index $n$. In the experimental conditions of this study, $Od$ is between 5.5 and 60. Plastic effects therefore predominate over viscous and inertia effects.

For a sphere, the ratio of plasticity effects to gravity effects is represented by:

$$Y = \frac{\tau_0}{gl\Delta\rho} \tag{5}$$

where $l$ and $\Delta\rho$ designate, respectively, the diameter of the sphere and the difference in density between the particles and the fluid. The smallest value of $Y$ beyond which the object is immobile is referred to as the stability criterion $Y_{\max}$. According to Beris et al.,[22] Chhabra,[23] Attapattu et al.,[24] Beaulne and Mitsoulis,[25] and Jossic and Magnin,[26] $Y_{\max}$ is between 0.048 and 0.111. The experimental parameters of this study give $Y = 808$; and the suspension is therefore very well stabilized. At rest, the spheres cannot sediment out simply under the effect of gravity.

Another dimensionless number needed to describe the flow is the ratio of the pipe diameter to the particle diameter: $\lambda = d/l \approx 8$.

## Experimental Set-Up

The experimental set-up used in this study consists of a reservoir supplying a horizontal cylindrical pipe at constant

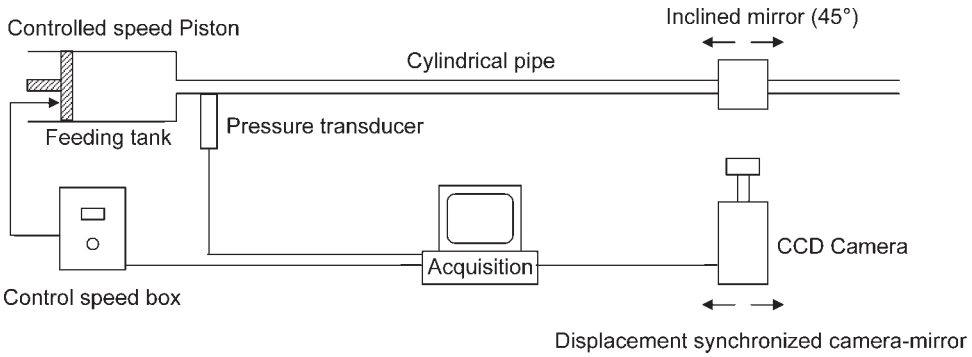


**Figure 2. Experimental set-up.**

velocity using a piston, Figure 2. The supply reservoir is made of transparent Plexiglas for viewing purposes and to ensure that the preparation is homogeneous. The piston is driven by a thrust system using a controlled-speed motor covering a range of very slow velocities between $10^{-7}$ and $10^{-3}$ m/s. The pipe is made of treated, transparent glass with a length $L = 580$ mm and a diameter $d = 5.5$ mm.

The pressure in the pipe is measured using a pressure sensor provided by Hirschmann. It can measure pressures with an accuracy of the order of 0.2 mbar. This pressure sensor is placed upstream of the pipe at a distance of six diameters after the outflow from the supply reservoir in order to avoid any perturbing effects. The pressure at the outlet from the pipe is atmosphere.

The phenomena observed are displayed using a camera-and-mirror system. This system uses a Sony CCD camera set perpendicular to the pipe in order to obtain a front view (plane containing the $X$ and $Z$ axes). To obtain a view from underneath the pipe (plane containing the $Y$ and $Z$ axes), we used a mirror inclined at 45°, Figure 3. The camera is joined to the mirror and can move along a rail in order to monitor the particles in the three dimensions of space along the flow. Pressures, velocities, and views are acquired on computer. All the experiments were performed in an air-conditioned room at 23°C ± 1°C.

## Material and Rheometry

The model suspensions used consist of a gelled fluid and solid particles. These are polystyrene spheres with a density $\rho = 1060$ kg/m$^3$. They were supplied by Marseille Chimie Berre l'Etang. A quasi-monodisperse population with a grain size distribution of between 680 and 700 $\mu$m was used. Little water is absorbed by the polystyrene (of the order of 1%).

Some of the particles were marked with a black line in order to quantify their rotation and distinguish the phenomena that may be generated in the flow.

The gel is a viscoplastic model fluid consisting of Carbopol and glucose. Carbopol 940 is manufactured by BF Goodrich,[27,28] and comes in the form of a white powder. The mass concentration of the Carbopol resin, 0.4% in this study, and the pH of the solution are used to adjust the yield-stress of the gel obtained. The glucose, supplied by Nigay S.A, has a Newtonian behavior. It is very viscous, pasty, and transparent. The Carbopol solution was mixed with 15% glucose in order to equalize the densities of the fluid and solid particles. The density of the fluid is $\rho_f = 1050$ kg/m$^3$, hence $\Delta\rho = 10$ kg/m$^3$.

After mixing the two fluids and neutralizing the mixture, the gel is aqueous, viscoplastic, transparent, and non-thixotropic with properties that remain stable in time. An antibacterial, sodium azide ($NaN_3$), was added at a concentration of 1 ml per liter of gel.

The yield stress and rheological parameters of the fluid were carefully characterized by controlled-speed rotating

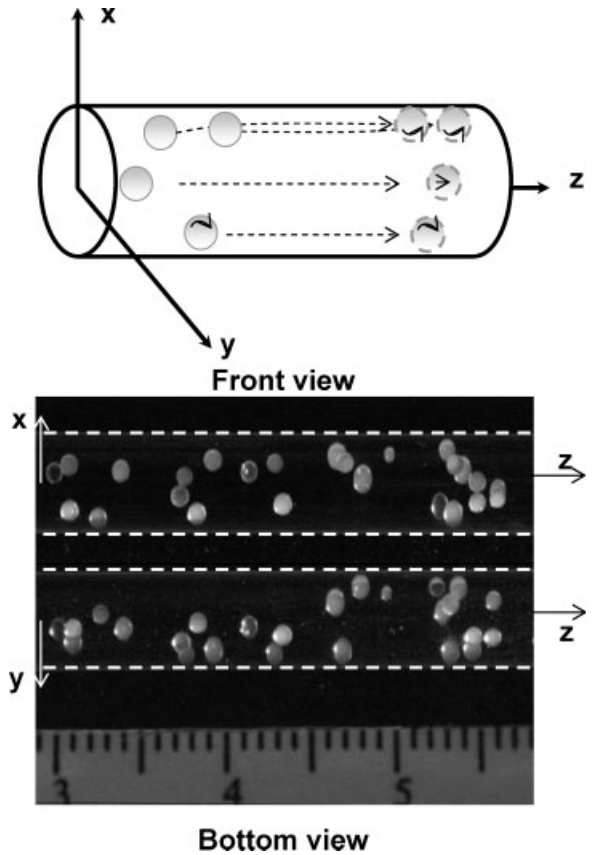


**Figure 3. Three-dimensional particles monitoring.**

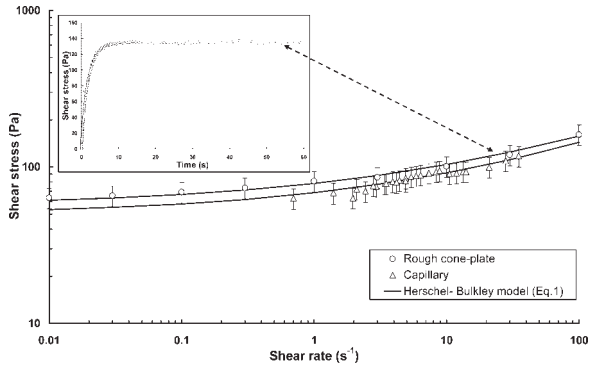


**Figure 4. Flow curve of Carbopol–glucose gel.**

Rheometrical measurements.

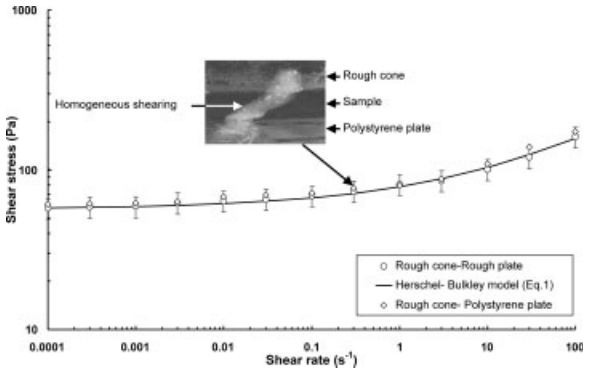


**Figure 5. Flow curve of Carbopol–glucose gel.**

Comparison between rheometrical and capillary measurements.

rheometry. An ARG2 rheometer from TA Instruments was used with a cone-plate cell in order to cover a wide range of shear rates between $10^{-4}$ $s^{-1}$ and $10^{2}$ $s^{-1}$. The surface state of the cone and plate were rough to prevent any slip at the surface. A solvent trap avoids the phenomenon of evaporation. Homogeneous shear within the bulk of the sample was checked by observation.[29,30]

To determine the gel's behavior when it is subjected to stress below its yield-stress and at low strain rates, harmonic oscillation tests were carried out to characterize changes in the viscoelastic parameters $G'$ and $G''$ as a function of the oscillation frequency. It can thus be shown that $G'$ and $G''$ are constant in the low-frequency domain. The elastic modulus $G'$ is about 16 times greater than the viscous modulus $G''$. The gel thus behaves like an elastic solid with an elastic modulus value of 250 Pa below its yield stress.

The flow curve, Figure 4, represents the change in shear stress in steady conditions as a function of the shear rate. Figure 4 also shows an example of the gel's response as a function of time to an imposed shear rate. These results are modeled by means of the Herschel-Bulkley equation (Eq. 1) with $\tau_0 = 56.6$ Pa, $k = 21.7$ Pa $s^{-0.33}$, and $n = 0.33$. The fluid's behavior is thus elastoviscoplastic. Piau[31] clearly shows the elastoviscoplastic behavior of carbopol gels. He presents a detailed analysis of the meso and macroscopic properties of these gels as well as the corresponding constitutive equations.

A characteristic time of the gel can be evaluated from the Herschel-Bulkley model and the elastic modulus $G'$: $t_m \sim (K/G')^{1/n}$. The characteristic time of the experiment is: $t_e \sim d/U$. The Weissenberg number can therefore be defined as $We = (K/G')^{1/n}\, U/d$. From the rheometrical results, it appears that the Weissenberg number ranges from $10^{-2}$ to $10^{-7}$. The Weissenberg number is very low in each case and the elastic effects can therefore always be neglected.

## Validation of Capillary Flow

The mechanical interactions of the particles with the fluid under shear can be determined by the slip at the interface that is commonly observed with yield-stress fluids.[25,26] It is therefore important to identify whether slip exists in these experimental conditions. Rheometric characterizations were therefore performed by using a cone-and-plate geometry and displaying the shear field (Figure 5). The rheometer was fitted with a rough cone to eliminate slip and a smooth polystyrene plate having the same properties as the solid particles used. Figure 5 shows that the views of the strain field do not reveal any slip at the cone and plate interfaces. Measurements carried out with the smooth polystyrene surfaces and rough surfaces eliminating slip give similar results.

Capillary flow is validated by comparing the flow curve obtained in rotating rheometry without slip and that obtained based on the flow rate-pressure measurements during pipe flow. Pipe flow was analyzed using capillary rheometry. As the Reynolds numbers are very small, the laminar velocity profile in the pipe is quickly established. End effects are negligible. The stress and shear rate at the wall, respectively, $\tau_w$ and $\dot{\gamma}_w$, are written as follows:

$$\begin{cases} \tau_w = \dfrac{R}{2}\dfrac{\Delta P}{L} \\ \dot{\gamma}_w = \dfrac{1}{4}\left(\dfrac{8u}{d}\right)\left[3 + \dfrac{dLnQ}{dLn\tau_w}\right] \end{cases} \tag{6}$$

where $Q$ designates the flow rate.

Figure 4 shows the measurements obtained in capillary flow and compares them with the rotating rheometry results. The measurements are similar. With capillary rheometry, no change in gradient characteristic of slip at the wall is

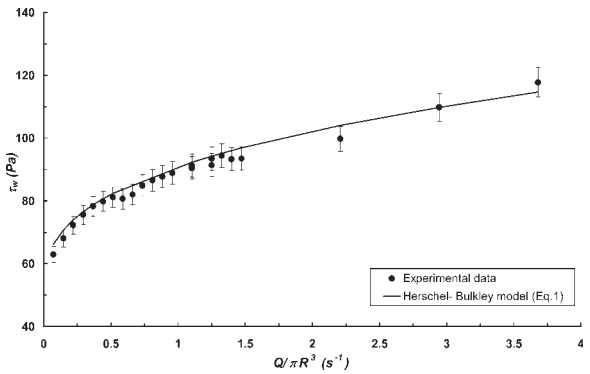


**Figure 6. Wall shear stress $\tau_w$ as a function of $Q/\pi R^3$.**

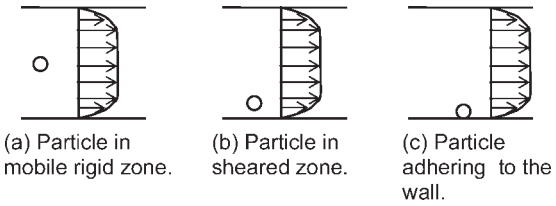


**Figure 7. Particle positions studied.**

detected. These results, presented in Figure 5, justify the assumption that there is no slip in the pipe. The Herschel-Bulkley model (Eq. 1) calibrated using the capillary rheometry measurements gives $\tau_0 = 49.8$ Pa, $k = 18.7$ Pa $s^{-0.35}$, and $n = 0.35$. The differences between the two methods do not exceed 15% and are within the uncertainties of the measurements.

To confirm the validation of pipe flow, we also compared the results obtained in this way with an analytical calculation of the flow of a viscoplastic fluid in a circular cylindrical pipe (Eq. 2). Figure 6 shows the change in shear stress at the wall $\tau_w$ as a function of $Q / \pi R^3$. The difference between the experimental results and calculation results does not exceed the uncertainty of the measurements, which is of the order of 5%.

## Experimental Results

Two volume concentrations of spherical particles were studied, $c_v = 1\%$ and 3%. Three cases were studied as a function of the position of the particles in the flow field, Figures 1 and 7.

The particle is completely within the mobile rigid zone or plug flow zone (Figure 7a).

The solid particle is completely or partly within the sheared zone (Figure 7b).

The particle is in contact with or is very close to the pipe wall and adheres to the wall (Figure 7c).

Figure 8 shows three photographs at different instants for $c_v = 1\%$. Two particles were monitored as a function of their position.

### *Particles situated in the mobile rigid zone (plug flow zone)*

In Figure 8a, particle no. 1 is situated more than three diameters from the upper wall of the pipe. In Figures 8b, c, the mark on this particle remains on the left side, even after it has moved more than 20 times its diameter. The motion of this sphere is therefore purely translational.

### *Particles situated completely or partly in the sheared zone*

Particle no. 2 is situated at less than its diameter from the wall. Figure 8b shows that after the particle has moved about twice its diameter, the mark has moved from the right to the top. Figure 8c shows that after the particle has moved about 12 times its diameter, the mark is at the bottom. In this case, the motion of the sphere is translational and rotational.

### *Particles adhering to the pipe wall*

The third case is represented in Figure 9. Particles situated very close to or in contact with the pipe wall do not move when the suspension begins to flow. Figure 9 illustrates the motion of two particles while the suspension is flowing. Particle no. 1 is situated at the wall, while particle no. 2, which acts as a reference, is situated far from the wall. In Figure 9a, the distance between these two spheres is less than one diameter. In Figure 9b the distance is more than four diameters. The first particle stays in the same position, while the second moves away. This phenomenon was observed several times.

To validate this result, this phenomenon was reproduced in a viscosimetric flow between the two planes of a rotating rheometer, Figure 10. The upper plate is rough and the lower is made of polystyrene. No slip was observed at the surface of the planes. The gap is equal to the radius $R$ of the pipe. The upper plate was marked in order to monitor the strain applied. The particle was placed against the wall using a needle and then a shear rate of 0.03 $s^{-1}$ was applied. Figure 10b shows that the particle remained in its initial position in spite of a strain of over 120%. As in the case of pipe flow, the particle adheres to the wall and can withstand the flow.

In conclusion, the following were observed as a function of the position of the particles in the flow:

- –translational motion of particles situated in the central zone of the pipe occupied by the plug flow zone,
- –rotational and translational motion of particles situated partly or fully in the sheared zone, and
- –no motion in the case of certain particles situated very close to the walls.

No migration of solid particles was recorded. The particles follow the stream lines, Figures 8 and 9.

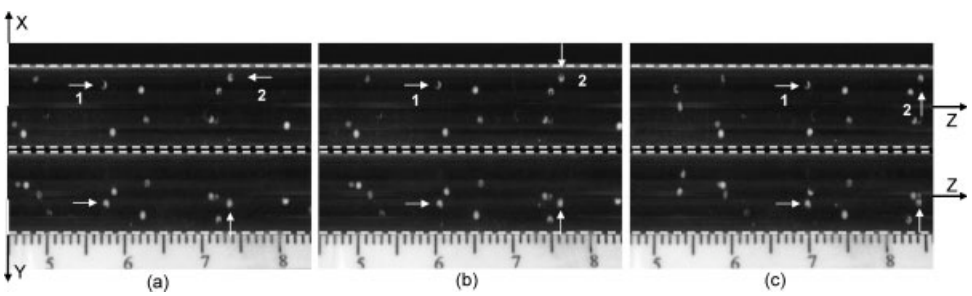


**Figure 8. Particle motion for $C_v = 1\%$; $u = 0.0028$ m $s^{-1}$; $Re = 0.0024$; $Od = 17.38$; $d/l = 8$; $\delta/d = 0.76$; $Y = 808$.**

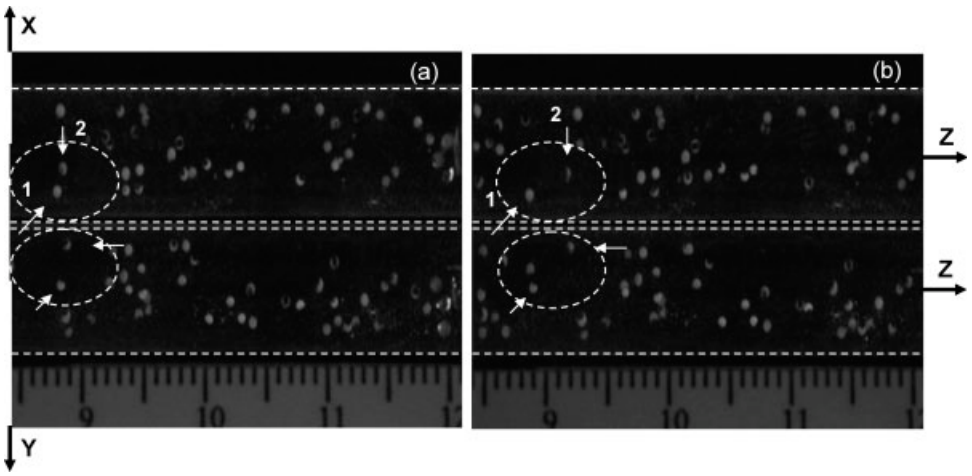


**Figure 9. Adherence of particles at the wall for $C_v$ = 3%; $u$ = 0.0004 m s$^{-1}$; $Re$ = 0.00011; $Od$ = 22.40; $d/l$ = 8; $\delta/d$ = 0.108; $Y$ = 808.**

## Discussion

### *Particles situated in the plug flow zone*

The physics of the phenomena described earlier can be explained by combining the experimental observations, Figures 8 and 9, with the analytical results of the calculation concerning the flow of a viscoplastic fluid in a cylindrical pipe, Figure 1. Particles situated in the plug flow zone move by translational motion, as the shear gradient in this zone is zero.

Figure 11 represents the change in the translation velocity of particles situated in the plug flow zone as a function of the Oldroyd number. The measured translation velocity $U_{TC}$ is made nondimensional by the maximum velocity of the particle-free gel $U_{max}$. Figure 11 also shows the change in the nondimensional average velocity $u$ of the particle-free gel. The particle velocity is representative of the velocity of the plug flow zone. It is of the same order of magnitude as the average velocity of the fluid $u$ in the absence of particles.

This may be explained by the fact that the particles have a significant volume in relation to the dimension of the plug flow zone. They do not behave as simple markers but modify the flow field. At high Oldroyd numbers, the translation velocity of the particles tends towards the velocity $U_{max}$ of the fluid alone, and the plug flow zone then tends to occupy the entire pipe. The translation velocity of the particles in the plug flow zone is independent of their position in it.

In the case of a Newtonian fluid, the formulae established by Greenstein and Happel[11] give $U_{TC}/U_{max} \approx 1$. This extreme case is shown in Figure 11.

If the fluid is of shear-thinning type, the experimental results of Gauthier et al.[18] give $U_{TC}/U_{max} \approx 0.76$ with a shear-thinning index of $n = 0.87$ and $\lambda = 8.5$, for a sphere positioned at $r = 0.503R$. For the sake of comparison, this value is also shown in Figure 11.

### *Particles situated completely or partly in the sheared zone*

Figure 12 shows the change in translation velocity, made nondimensional by the maximum velocity of the particle-free gel in the pipe, as a function of the Oldroyd number. By way of comparison, the values obtained in the case of a Newtonian fluid and a shear-thinning fluid is also shown in this figure. The formulae established by Greenstein and Happel[11] give $U_{TW}/U_{max} \approx 0.22$ for a particle very close to the wall. In the case of a shear-thinning fluid, the experimental

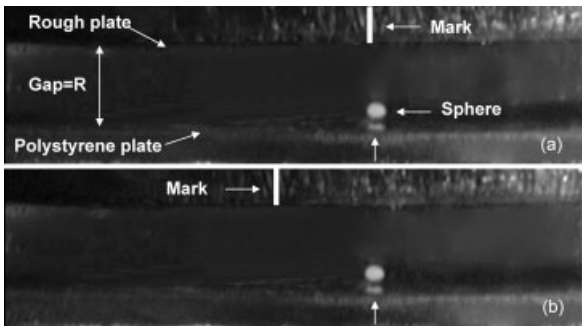


**Figure 10. Confirmation of adherence at the wall of particles in a rheometer; $\gamma$ = 200%, $\dot{\gamma}$ = 0.03 s$^{-1}$, steady state is reached.**

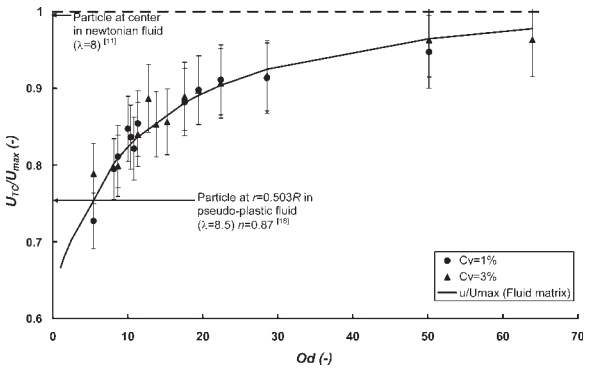


**Figure 11. Dimensionless translation velocity as a function of Oldroyd number for particles located in the mobile rigid zone.**

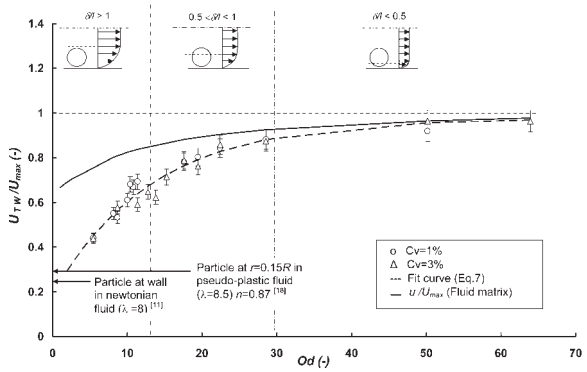


**Figure 12. Dimensionless translation velocity as a function of Oldroyd number for particles located in the sheared zone.**

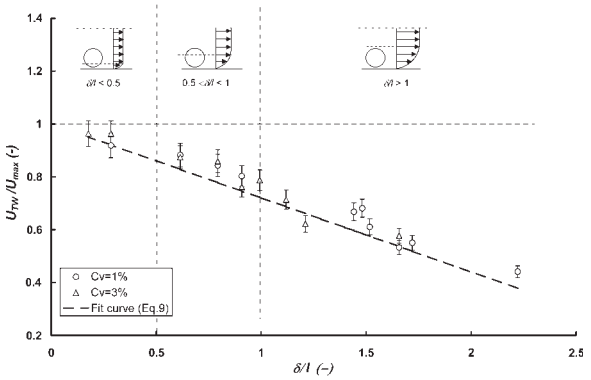


**Figure 14. Dimensionless translation velocity as a function of the size of the sheared zone.**

results of Gauthier et al.[18] give $U_{TW}/U_{max} \approx 0.282$ for a particle situated at $r = 0.815R$, with $n = 0.87$ and $\lambda = 8.5$.

Figure 13 shows the change in rotation velocity, made nondimensional by the ratio of the maximum velocity of the particle-free gel in the pipe to the thickness of the sheared zone, as a function of the Oldroyd number. As an initial approximation, it may be assumed that the ratio of the maximum velocity of the particle-free gel in the pipe to the thickness of the sheared zone gives a good estimation of the shear rate in the sheared zone.

It should be recalled that in the case of a Newtonian fluid, the rotation velocity of a particle is equal to half the shear rate.

Figures 14 and 15 show, respectively, the change in the dimensionless translation and rotation velocities as a function of the ratio of the thickness of the sheared zone to the diameter of the spheres $\delta/l$. For the two-particle volume concentrations considered, 1% and 3%, the differences are less than the measurement uncertainties. These suspensions are dilute and the difference in concentration does not imply any change in behavior during flow.

In general, these figures show that when the Oldroyd number increases, i.e. when the thickness of the sheared zone decreases, the translation velocity increases and tends towards the maximum velocity of the particle-free gel. In contrast, the rotation velocity decreases until it is cancelled.

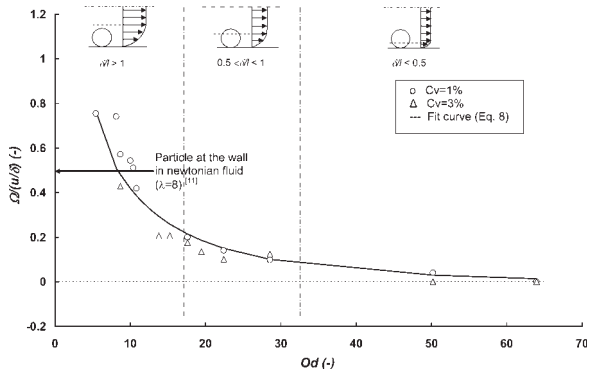


**Figure 13. Dimensionless rotation velocity as a function of Oldroyd number for particles located in the sheared zone.**

These variations are directly linked to the increase in the moving rigid zone, which invades an increasingly large proportion of the pipe. They can be explained by the positions of the particles in relation to the sheared zone.

At low Oldroyd numbers, when $\delta/l > 1$, the particle is situated completely in the sheared zone. It is therefore completely subject to nonzero shear gradients. The translation velocity varies considerably with the number. There are considerable differences in comparison with the average velocity of the particle-free gel at the lowest Oldroyd numbers. These differences are justified by the presence of the particle, which is of similar size to the diameter of the pipe, and therefore considerably perturbs the particle-free velocity field.

When the Oldroyd number increases, the thickness of the sheared zone becomes similar to the diameter of the sphere. The particle is then partly in the rigid zone. Part of the sphere is then influenced by shear in the sheared zone, while the other is situated in the rigid zone. There is thus a decrease in the rotation velocity due to a reduction in the torque applied to the particle, as the shear gradients in the rigid zone are very small or nil. In contrast, the translation velocity increases under the influence of the mobile rigid zone. This increase is not sufficient for the particle to reach average velocity.

At high Oldroyd numbers, the thickness of the sheared zone becomes very small in comparison with the diameter of the sphere. The particle is situated essentially in the rigid

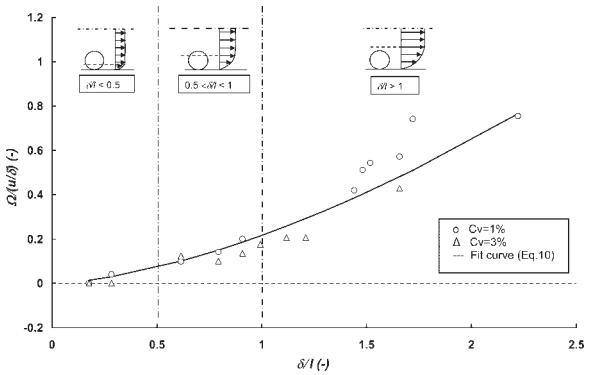


**Figure 15. Dimensionless rotation velocity as a function of the size of the sheared zone.**

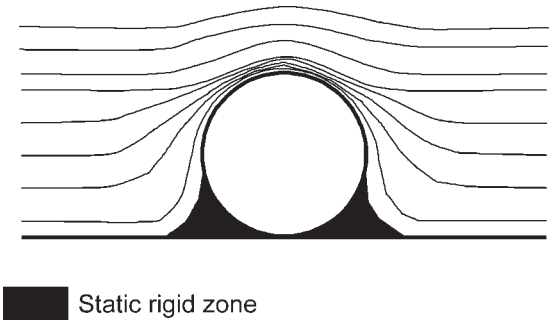


**Figure 16. Flow configuration around a sphere adhering to a wall for very low Reynolds numbers.**

zone. Motion is mainly governed by the rigid zone. The translation velocity of the particles increases until it tends towards the maximum velocity $U_{max}$ of the particle-free gel. The particle rotation velocity decreases until it stops. The very low shear gradients in the rigid zone exert only a small torque on the particle, insufficient to cause it to rotate.

The changes in translation and rotation velocities as a function of the Oldroyd number can be modeled respectively by:

$$\frac{U_{TW}}{U_{max}} = 1 - 0.79e^{-Od/13.3} \tag{7}$$

$$\frac{\Omega}{U_{max}/\delta} = \frac{4.5}{Od^{1.11}} \tag{8}$$

The changes in translation and rotation velocities as a function of the thickness of the sheared zone can be modeled respectively by:

$$\frac{U_{TW}}{U_{max}} = 1 - 0.28\frac{\delta}{l} \tag{9}$$

$$\frac{\Omega}{U_{max}/\delta} = 0.2\left(\frac{\delta}{l}\right)^{1.54} \tag{10}$$

### *Particles adhering to the pipe wall*

The particles adhering to the pipe wall, Figures 9 and 10, are submitted to viscoplastic forces which depend on the yield-stress and the gap between the sphere ant the wall. These forces have to be exceeded to allow the motion of the spheres. This phenomenon may be explained by the fluid's plasticity which generates static rigid zones around the particle that hold it to the wall. Figure 16 gives a schematic representation of the static rigid zones assumed to hold the solid particles to the pipe wall.

So far, this phenomenon has received little interest in the literature. In the case of the squeeze flow, Adams et al.,[32] Sherwood and Durban,[33,34] and Meeten[35–37] studied the change in the squeezing force of yield stress fluids in different geometries: between two parallel plates, between a flat surface and concave and convex spherical surfaces. They demonstrated the existence of a yield force that has to be overcome in order for an object to move away from or towards a flat wall.

## Conclusions

This study deals with the mechanisms governing the dynamics of rigid spheres suspended in a viscoplastic fluid flowing in a cylindrical pipe. The flows have low Reynolds numbers and high Oldroyd numbers. Plastic effects therefore predominate over viscous and inertia effects. The suspensions used are well stabilized and gravity effects are negligible. In these experimental conditions no migration of solid particles was recorded; the particles follow the streamlines. The dynamics of a particle depends on its position in the pipe. Particles situated in the middle of the pipe, in the plug flow zone, move only by translation. Particles situated near the walls, in the shear flow zone, have both a translational and rotational motion. Certain particles very close to the walls are static and do not move in spite of the flow. The translation velocity of particles situated in the plug flow zone is independent of their position in this zone. The translation and rotation velocities of particles situated partly or completely in the sheared zone depend on their position in relation to the sheared zone. The change in translation and rotation velocities was quantified as a function of the Oldroyd number and thickness of the sheared wall zone.

The observations provide new basic knowledge concerning the flow of suspensions in viscoplastic fluids. They open up new prospects for future modeling studies.

## Notation

$D$ = diameter of the supply reservoir (m)
$d$ = diameter of the pipe (m)
$l$ = diameter of the particles (m)
$f$ = frequency (Hz)
$g$ = acceleration due to gravity (m $s^{-2}$)
$G'$ = elastic modulus (Pa)
$G''$ = viscous modulus (Pa)
$K$ = consistency index (Pa $s^n$)
$L$ = length of the pipe (m)
$n$ = power-law index (−)
$P$ = pressure (Pa)
$Q$ = flow rate ($m^3$ $s^{-1}$)
$r_s$ = radius of the plug flow zone (m)
$R$ = radius of the pipe (m)
$U$ = velocity (m $s^{-1}$)

### *Greek letters*

$\tau$ = shear stress (Pa)
$\tau_0$ = yield stress (Pa)
$\dot{\gamma}$ = shear rate ($s^{-1}$)
$\gamma$ = strain (%)
$\rho$ = density (kg $m^{-3}$)
$\delta$ = thickness of the sheared zone (m)
$\Omega$ = particle rotation velocity (rad $s^{-1}$)

### *Dimensionless numbers*

$Re$ = Reynolds number
$Od$ = Oldroyd number
$Y$ = ratio of yield stress to gravity effects
$Y_{max}$ = stability criterion

### *Indices*

C = center
P = particle
T = transfer
W = wall
max = maximum

## Acknowledgments

The authors thank Pr. Jean-Michel Piau for his helpful comments and the referees for thorough and detailed remarks.

## Literature Cited

1. Jossic L, Briguet A, Magnin A. Segregation under flow of objects suspended in a yield stress fluid and NMR imaging visualisation. *Chem Eng Sci*. 2002;57:409–418.
2. Jossic L, Magnin A. Structuring under flow of suspensions in gel. *AIChE J*. 2004;50:2691–2696.
3. Jossic L, Magnin A. Structuring of gelled suspensions flowing through a sudden three-dimensional expansion. *J Non-Newtonian Fluid Mech*. 2005;127:201–212.
4. Segré G, Silberberg A. Behaviour of macroscopic rigid spheres in Poiseuille flow. II. Experimental results and interpretation. *J Fluid Mech*. 1962;14:136–157.
5. Brenner H, Happel J. Slow viscous flow past a sphere in a cylindrical tube. *J Fluid Mech*. 1958;4:195–213.
6. Happel J, Brenner H. *Low Reynolds Number Hydrodynamics*. Prentice-Hall, The Hague: Martinus Nijhoff Publishers, 1965.
7. Goldsmith HL, Mason SG. The flow of suspensions through tubes. I. Single spheres, rods, and discs. *J Colloid Sci*. 1962;17:448–476.
8. Denson CD, Christiansen EB, Salt DL. Particle migration in shear fields. *AIChE J*. 1966;12:589.
9. Brenner H. Hydrodynamic resistance of particles at small Reynolds numbers. *Adv Chem Eng*. 1966;6:287–438.
10. Cox RG, Brenner H. The lateral migration of solid particle in Poiseuille flow. I. Theory. *Chem Eng Sci*. 1968;23:147.
11. Greenstein T, Happel J. Theoretical study of the slow motion of sphere and a fluid in a cylindrical tube. *J Fluid Mech*. 1968;34:705–710.
12. Cox RG, Mason SG. Suspended particles in fluid flow through tubes. *Annu Rev Fluid Mech*. 1971;3:291–316.
13. Feng J, Hu HH, Joseph DD. Direct simulation of initial value problems for motion of solid bodies in a Newtonian fluid. I. Sedimentation. *J Fluid Mech*. 1994;95:261.
14. Matas JP, Morris JF, Guazzelli E. Transition to turbulence in particulate pipe flow. *Phys Rev Lett*. 2003;90:014501.
15. Matas JP, Morris JF, Guazzelli E. Inertial migration of rigid spherical particles in Poiseuille flow. *J Fluid Mech*. 2004;515:171–195.
16. Matas JP, Morris JF, Guazzelli E. Lateral force on a sphere. *Oil Gas Sci Technol Rev IFP*. 2004;59:59–70.
17. Karnis A, Mason SG. Particle motion in sheared suspensions. XIX. Viscoelastic media, *Trans Soc Rheol*. 1966;10:571.
18. Gauthier F, Goldsmith HL, Mason SG. Particle motions in non-newtonian media. II. Poiseuille flow. *Trans Soc Rheol*. 1971;15:297–330.
19. Scott-Blair GW. *An Introduction to Industrial Rheology*. Philadelphia: P Blakiston's Son and Co, 1938.
20. Oldroyd JGT. A rational formulation of the equations of plastic flow for a Bingham solid. *Proc Camb Philos Soc*. 1947;43:100–105.
21. Oldroyd JGT. Two-dimensional plastic flow of a Bingham solid. A boundary-layer theory for slow motion. *Proc Camb Philos Soc*. 1947;43:383–395.
22. Beris AN, Tsamopoulos JA, Armstrong RC, Brown RA. Creeping motion of a sphere through a Bingham plastic. *J Fluid Mech*. 1985;158:219–244.
23. Chhabra RP. *Bubbles, Drops and Particles in Non-Newtonian Fluids*. Boca Raton, Florida: CRC Press, 1993.
24. Atapattu DD, Chhabra RP, Uhlherr PHT. Creeping motion in Herschel-Bulkley fluids: flow field and drag. *J Non-Newtonian Fluid Mech*. 1995;59:245–265.
25. Beaulne M, Mitsoulis E. Creeping motion of a sphere in tubes filled with Herschel-Bulkley fluids. *J Non-Newtonian Fluid Mech*. 1997;72:55–71.
26. Jossic L, Magnin A. Drag and stability of objects in a yield stress fluid. *AIChE J*. 2001;47:2666–2672.
27. BF Goodrich. *Literature, Carbopol Resins Handbook*. Cleveland, OH, 1997.
28. BF Goodrich. *Literature, Carbopol Resins Handbook*. Cleveland, OH, 1998.
29. Magnin A, Piau JM. Shear rheometry of fluids with a yield stress. *J Non-Newtonian Fluid Mech*. 1987;23:91–106.
30. Magnin A, Piau JM. Cone and plate rheometry of yield stress fluids. Study of an aqueous gel. *J Non-Newtonian Fluid Mech*. 1990;36:85–108.
31. Piau JM. Carbopol gels: elastoviscoplastic and slippery glasses made of individual swollen sponges: meso- and macroscopic properties, constitutive equations and scaling laws. *J Non-Newtonian Fluid Mech*. 2007;144:1–29.
32. Adams MJ, Edmondson B, Caughey DG, Yahya R. An experimental and theoretical study of the squeeze-film deformation and flow of elastoplastic fluids. *J Non-Newtonian Fluid Mech*. 1994;51:61–78.
33. Sherwood JD, Durban DM. Squeeze flow of a power-law viscoplastic solid. *J Non-Newtonian Fluid Mech*. 1996;62:35–54.
34. Sherwood JD, Durban DM. Squeeze-flow of a Herschel-Bulkley fluid. *J Non-Newtonian Fluid Mech*. 1998;77:115–121.
35. Meeten GH. Yield stress of structured fluids measured by squeeze flow. *Rheol Acta*. 2000;39:399–408.
36. Meeten GH. Squeeze flow between plane and spherical surfaces. *Rheol Acta*. 2001;40:279–288.
37. Meeten GH. Flow of soft solids squeezed between planar and spherical surfaces. *Rheol Acta*. 2005;44:563–572.

*Manuscript received July 5, 2007, and revision received Dec. 20, 2007.*